Advanced Physical Research
Vol.8, No.1, 2026, pp.162-172
https://doi.org/10.62476/apr.81162

DENSITY FUNCTIONAL THEORY PERSPECTIVE ON Zn ADSORPTION ON THE $NiFe_2O_4$ (001) SURFACE

Saida Mammadova[1,2,3*], **Amida Sadigova**[1], **Afet Kerimova**[1], **Billure Hajiyeva**[4], **Vusala Mammadova**[5]

[1]Institute of Physics, Ministry of Science and Education of Azerbaijan, AZ1143, Baku, Azerbaijan
[2]Faculty of Mathematics, Khazar University, AZ1096 Baku, Azerbaijan
[3]Department of Higher Mathematics, Baku Business University, Baku, Azerbaijan
[4]Nakhichevan State University, Nakhichevan, Azerbaijan
[5]Baku State University, Baku, Azerbaijan

Abstract. In this study, the structural and electronic properties of $NiFe_2O_4$ were investigated with a focus on the effects of Zn adsorption on the (001) surface. Zn adsorption on the $NiFe_2O_4$ (001) surface was explored at three different sites (top, bridge, and hollow), and the resulting adsorption energies are in good agreement with previously reported values for analogous systems. The adsorption of Zn significantly alters the crystal structure and the electronic band structure, affects the magnetic characteristics of the material. Density of states analysis demonstrates that Zn adsorption on $NiFe_2O_4$ (001) surface is a strong spin asymmetry between the spin-up and spin-down channels, indicating exchange splitting and long-range magnetic order. These findings provide valuable insights into the role of Zn adsorption in tuning the electronic and magnetic properties of $NiFe_2O_4$, highlighting its potential for surface-engineered spintronic and catalytic applications.

Keywords: $NiFe_2O_4$, adsorption energy, density functional theory, structural and electronic properties.
Corresponding author: Saida Mammadova, Institute of Physics, Ministry of Science and Education of Azerbaijan, AZ1143 Baku, Azerbaijan, e-mail: *memmedova_seide.fiz@mail.ru*
Received: 17 October 2025; Revised: 28 November 2025; Accepted: 5 December 2025; Published: 18 February 2026.

1 Introduction

Since its opening, $NiFe_2O_4$ has generated considerable interest among scientists owing to its distinctive optoelectronic and magnetic characteristics. One of the important preferences of magnetic nanoparticles in wastewater treatment is their magnetic separability, which enables quickly and efficient removal from aqueous systems following pollutant adsorption. Among them, the most widely studied and used are ferrites - nanoparticles consisting mainly of iron oxides and ions of other metals (Nnadozie & Ajibade, 2020; Sidorowicz et al., 2024). Their high chemical stability under variable pH, temperature, and chemical conditions makes them especially suitable for harsh wastewater environments, as it helps conserve structural integrity and minimizes the release of potentially harmful ions (Kefeni & Mamba, 2020; Kefeni et al., 2017). Ferrites such as magnetite (Fe_2O_4) and nickel ferrite ($NiFe_2O_4$) exhibit strong magnetic properties that enable effective separation from aqueous media using external magnetic fields (Zohrabi, 2024; Nithya et al., 2021). In addition, doping ferrites with transition metals such as nickel can improve

their saturation magnetization, leading to improved separation efficiency (Salih & Mahmood, 2023). These properties second their application in continuous flow systems by facilitating faster nanoparticle recovery and decreasing energy consumption, thereby improving the overall sustainability and feasibility of the treatment process.

A wide variety of adsorbent materials have been investigated in recent years for the removal of water pollutants (Adam et al., 2022). Magnetic ferrite nanoparticles are of significant interest due to their intrinsic magnetic properties that enable useful separation from aqueous media. These nanoparticles possess high porosity and a large specific surface area, combined with low cost and facile surface functionalization, which collectively contribute to their enhanced selectivity toward target contaminants (Kefeni et al., 2017). Due to their distinctive physicochemical properties (Leonel et al., 2021), including efficient ultraviolet and visible light absorption, exceptional thermal stability, and pronounced magnetic responsiveness, magnetic nanoparticles have been extensively explored for a broad range of applications encompassing biomedicine (Srinivasan et al., 2018), energy storage (Srinivasan et al., 2018), sensing technologies (Goncalves et al., 2022), photocatalytic water splitting (Farhan et al., 2023), and wastewater treatment (Kefeni & Mamba, 2020).

The utilization of nanostructured materials as adsorbents has attracted substantial research interest owing to their exceptionally high specific surface area and superior adsorption performance. Among the various nanomaterials investigated-including zero-valent metals, metal oxides, carbon-based nanomaterials, and magnetic nanocomposites. Their inherent magnetic properties, combined with a high density of active functional groups, confer distinct advantages over conventional nonmagnetic adsorbents. Conventional adsorbents frequently encounter limitations such as low adsorption capacity, poor selectivity, challenging recovery processes, and the risk of secondary pollution. The $NiFe_2O_4$ (001) surface was studied due to its thermodynamic stability, low surface energy, and experimental relevance. This surface demonstrates both tetrahedral and octahedral cation sites, providing multiple active adsorption sites for Zn atoms. Moreover, the (001) orientation is commonly observed in ferrite thin films, making it a suitable model for exploring adsorption-induced structural and electronic modifications.

2 Model and Calculation Method

Ab-initio calculations based on the density functional theory with the Quantum ATK simulation package have been performed in order to gain further insights into the electronic structure and energetics for Zn adsorbed on $NiFe_2O_4$ (001) surface (Asadov et al., 2023, 2024, 2025). The $NiFe_2O_4$ (001) surface was modeled utilizing an asymmetric slab consisting of 8 atomic layers with a vacuum thickness of 20 Å along the surface normal. The bottom layers were fixed to bulk positions, while the upper layers and the Zn adatom were fully relaxed. A dipole correction was applied along the z direction. To facilitate clearer visualization and enable a direct comparison of the adsorption energies, the present study focuses exclusively on the (001) surface of the $NiFe_2O_4$ compound.

Perdew-Burke-Ernzerhof parameterization spin generalized gradient approximation (SGGA) have used for the approximate treatment of the electron exchange and correlation, together with a plane-wave cutoff energy of 150 Ry. The primitive cell of $NiFe_2O_4$ was relaxed and optimized with force and stress tolerances of 0.01eV/Å and 0.01eV/Å^3, respectively. In the irreducible part of the Brillouin zone, the k-point integration was performed on 3×3×1 Monkhorst-Pack mesh. To characterize the localized 3d electrons in $NiFe_2O_4$, the DFT+U method was employed with Hubbard parameters of U = 5.0 eV for Fe 3d states and U = 6.0 eV for Ni 3d states. Spin polarization was entered in all calculations, and magnetic moments were allowed to relax self-consistently. Taking into account the electron spin in the $NiFe_2O_4$ -Zn structure is important because the interaction of the magnetic moment associated with the spin with the magnetic field created by the orbital rotation of the electron makes a certain contribution to the total energy

of the system. Taking this into account, the spin-polarized generalized gradient approximation SGGA was used to calculate the energy, which depends, in particular, on the charge and spin density d of nickel electrons. That is, the calculations of the energy $NiFe_2O_4$ -Zn structures included spin-dependent exchange correlation functionals.

3 Results and discussion

3.1 Atomic and Electronic Structure

Spinel ferrites are among the oldest magnetic materials, second only to metallic iron, which originates mainly from meteorite sources. The term *spinel* refers to their characteristic crystal structure, is similar to that of the natural mineral $MgAl_2O_4$. Spinel ferrites are generally described by the chemical formula AB_2O_4, where 'A' demonstrates a divalent cation and 'B' a trivalent cation (Narang & Pubby, 2021). Depending on the distribution of cations between the octahedral and tetrahedral sites, spinels are classified as either normal or inverse spinels. In a normal spinel structure, the divalent cations (A^{2+}) occupy the tetrahedral (A) sites, while the trivalent cations (B^{3+}) occupy the octahedral (B) sites exclusively. In contrast, an inverse spinel structure is characterized by the divalent cations (A^{2+}) occupying half of the (B) sites, where the trivalent cations (B^{3+}) are equally divided between the (A) sites and the remaining octahedral (B) sites.

The Figure 1 a) displays a crystal structure of $NiFe_2O_4$, a well-known spinel-type material with a cubic symmetry, typically belonging to the $Fd\bar{3}m$ space group. The structure is face-centered cubic (fcc) with lattice parameter ≈ 5.996281Å. The atomic structure of nickel ferrite adopts an inverse spinel configuration, where Ni^{2+} ions occupy (B) sites, while Fe^{3+} ions are distributed between (A) and (B) sites. In the inverse spinel configuration of $NiFe_2O_4$:

$$(Fe^{3+})_A[Ni^{2+}, Fe^{3+}]_B O_4.$$

In $NiFe_2O_4$, the valence band is mainly formed by O-2p states hybridized with Fe-3d orbitals, indicating strong p-d interaction in the spinel lattice. The electronic states near the Fermi level are dominated by Fe-3d and Ni-3d contributions, while the conduction band originates primarily from Fe-3d states with minor Ni-3d participation. This electronic structure demonstrates that the fundamental electronic and magnetic behavior of $NiFe_2O_4$ is governed by the localized d electrons of Fe and Ni ions, which control exchange interactions and magnetic ordering.

In this study, the $NiFe_2O_4$ (001) surface was modeled to investigate the adsorption behavior of a Zn atom. Initially, we considered the zinc atom site on top of Ni (TS), the Zn bridging site of the Ni-Ni bond (BS), and the hollow site in the lattice voids (HS). (Figure 1 b,c,d). Then structural optimization was performed using density functional theory to determine the most energetically favorable configuration. After relaxation, Zn exhibited strong binding to the surface, accompanied by slight local distortion of surrounding atoms. These changes suggest charge redistribution and surface reconstruction in response to Zn adsorption.

In this work, evaluate the influence of Zn adsorption on the electronic properties of the $NiFe_2O_4$ (001) surface, the total density of states (DOS) was calculated for the bridge (BS), top (TS), and hollow (HS) adsorption sites (Figure 2). The DOS profiles of all three configurations retain the general features of the pristine $NiFe_2O_4$ surface but exhibit distinct variations near the Fermi level, confirming site-dependent perturbations in electronic structure.

Zn adsorption introduces subtle shifts and intensity changes in the -4 to 0eV range, associated with hybridization between Zn 3d orbitals and surface O 2p and Fe 3d states. The hollow site configuration displays slightly higher DOS near the Fermi level, implying stronger electronic coupling and potential reduction in the effective band gap. This suggests that Zn atoms preferentially adsorbed at hollow sites may enhance the surface's electronic conductivity, an effect beneficial for catalytic and magnetic performance tuning. From the DOS Figure 2, it

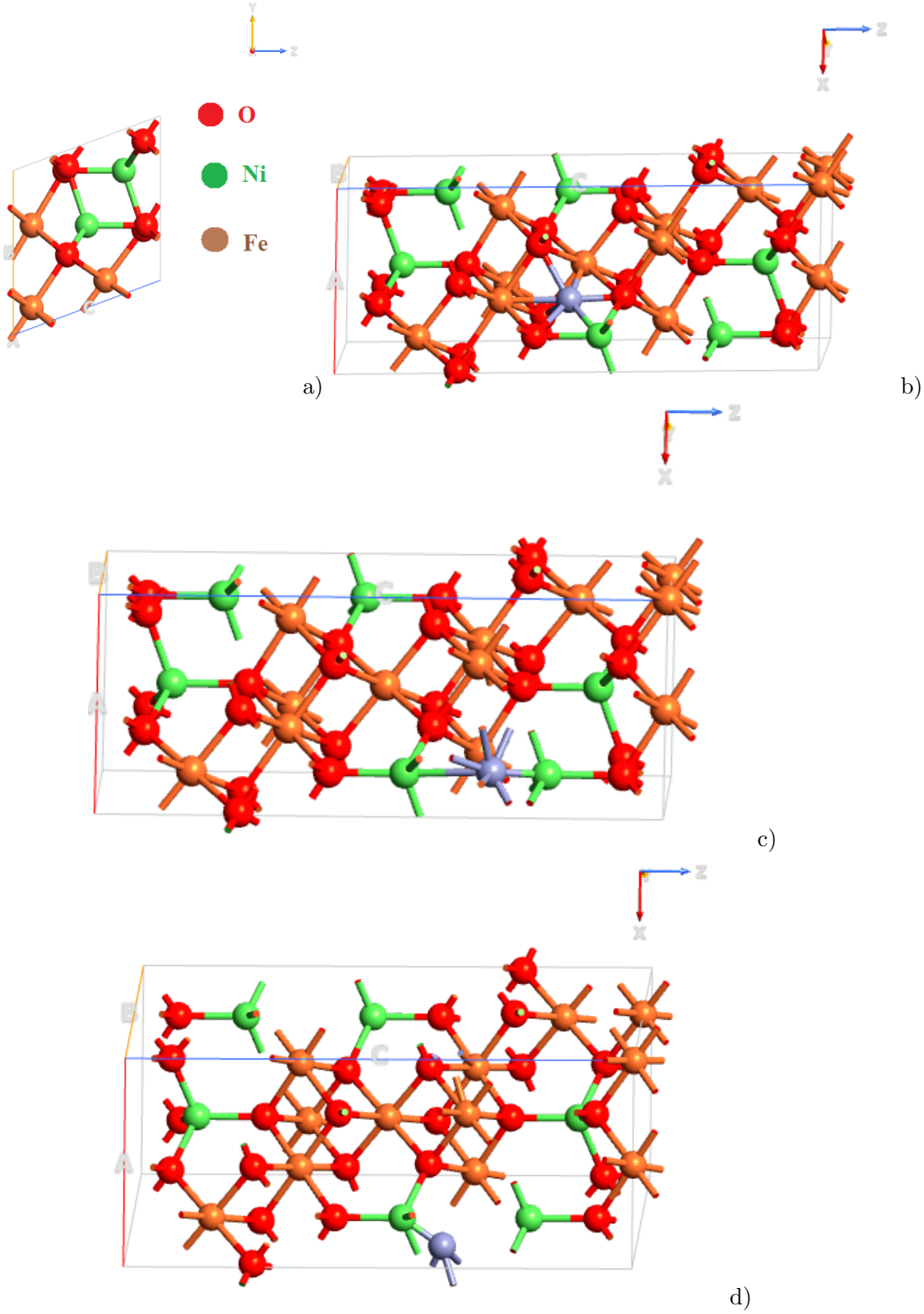

Figure 1: Atomic structure: (a) $NiFe_2O_4$ spinel crystal structure; adsorption configuration of a Zn atom on the $NiFe_2O_4$ (001) surface: (a) top site with Ni, (b) bridge side with Ni-Ni bond, (c) hollow site in the lattice voids. The Ni, Fe, O, and Zn atoms are depicted in green, brown, red, and grey, respectively.

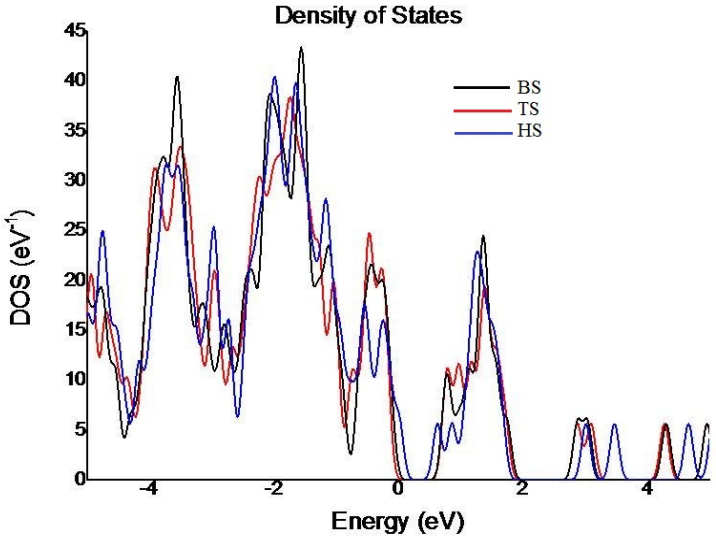

Figure 2: Calculated DFT SGGA of spin-allowed density of states of the Zn adsorption on the $NiFe_2O_4$ (001) surface: (a) bridge (BS, black), (b) top (TS, red), and (c) hollow (HS, blue).

can be seen that both the spin-up and spin-down states cross the Fermi level at non-zero values. This indicates that our sample exhibits metallic behavior. The metallic behavior arises from surface-induced electronic states and Zn-induced modification of Fe 3d-O 2p hybridization. Surface symmetry breaking and charge redistribution introduce partially filled states at the Fermi level in both spin channels, leading to finite density of states at E_F and metallic conductivity.

Partial density of states analysis confirms that Zn 3d states are mainly localized between -6 and -2 eV, overlapping with O 2p and Fe 3d states, consistent with covalent-type bonding behavior. A minor contribution from Ni 3d orbitals is also detected near the Fermi level, indicating limited but significant Ni-Zn coupling. The partial charge transfer and hybridization introduce new shallow electronic states near the Fermi level, particularly for the hollow-site configuration. These findings suggest that Zn adsorption induces local electronic rearrangement and enhances the surface's semiconducting character, which could influence the catalytic and magnetic properties of $NiFe_2O_4$. Overall, the DOS analysis confirm that Zn adsorption on $NiFe_2O_4$ (001) surface is a strong spin asymmetry between the spin-up and spin-down channels, indicating exchange splitting and long-range magnetic order.

Figure 4 shows the electronic band structure of $NiFe_2O_4$ calculated using the DFT+U method, with Hubbard parameters of U = 5.0 eV for Fe-3d states and U = 6.0 eV for Ni-3d states. The calculated band gap (E_g) of inverse spinel $NiFe_2O_4$ is 2.82 eV, which is in good agreement with the experimental value of 2.74 eV (direct band gap) reported in (Dileep et al., 2014)

3.2 Adsorption Energetics

The electron configuration of zinc [Ar]3d104s2 has only one oxidation state, Zn^{2+}, which has a filled d-shell. Zn^{2+} can bind various ligands and undergo ligand exchange reactions. These issues are not discussed in this article; for DFT calculations of zinc adsorption on the $NiFe_2O_4$ (001) surface, it is sufficient to use a neutral zinc atom. This is because zinc acquires a charge through exchange reactions in the $NiFe_2O_4$ (001)- Zn system.

The adsorption energies E_{ads}^{Zn} of a Zn atom on a $NiFe_2O_4$ (001) surface is calculated as follow:

$$E_{ads}^{Zn} = E[Zn\ /NiFe_2O_4](001)\ - E[Zn] - E[NiFe_2O_4](001)$$

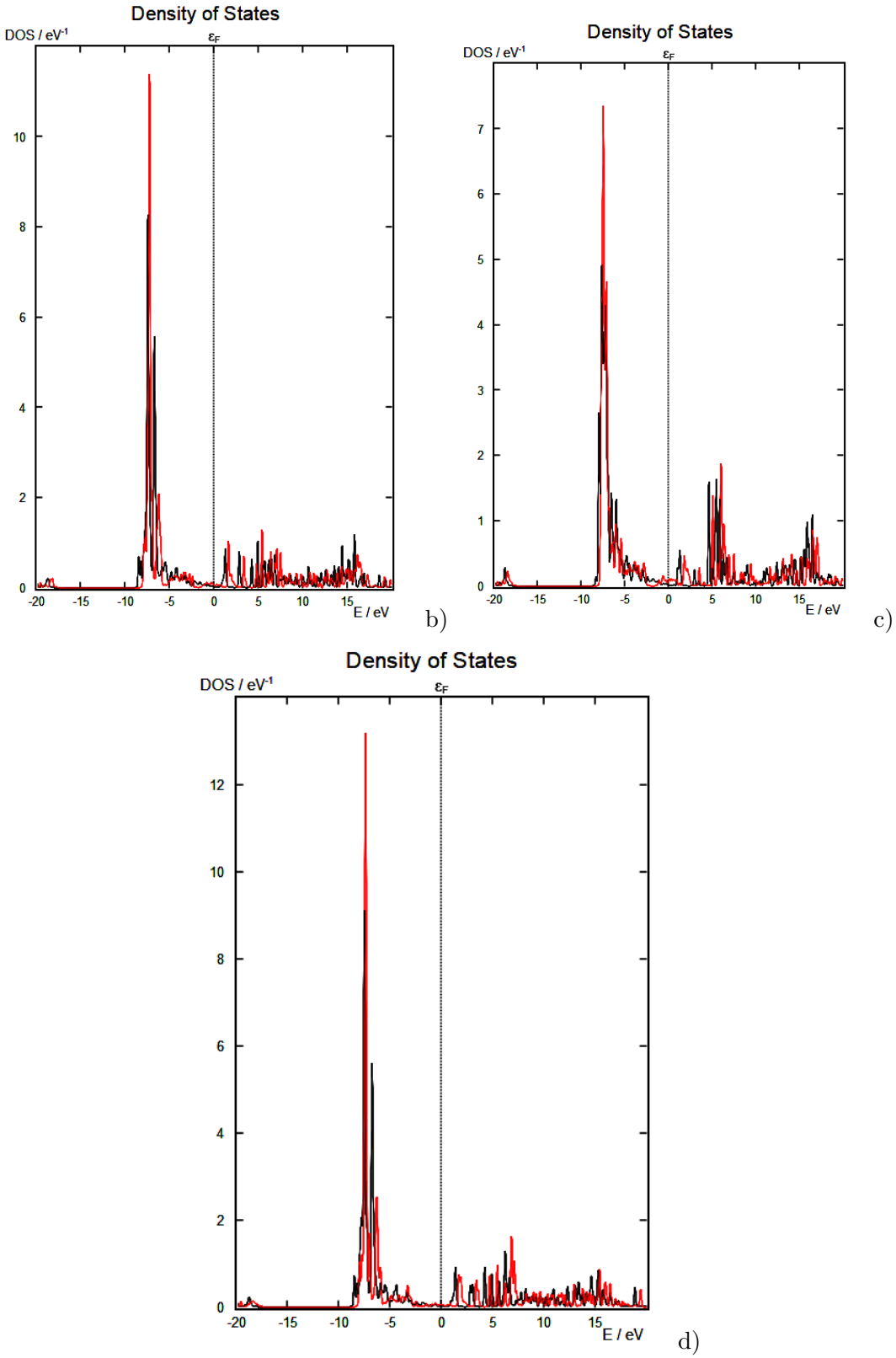

Figure 3: Partial density of states (PDOS) of the $NiFe_2O_4$ (001) surface with Zn adsorbed at three different sites: (a) bridge, (b) top, and (c) hollow.

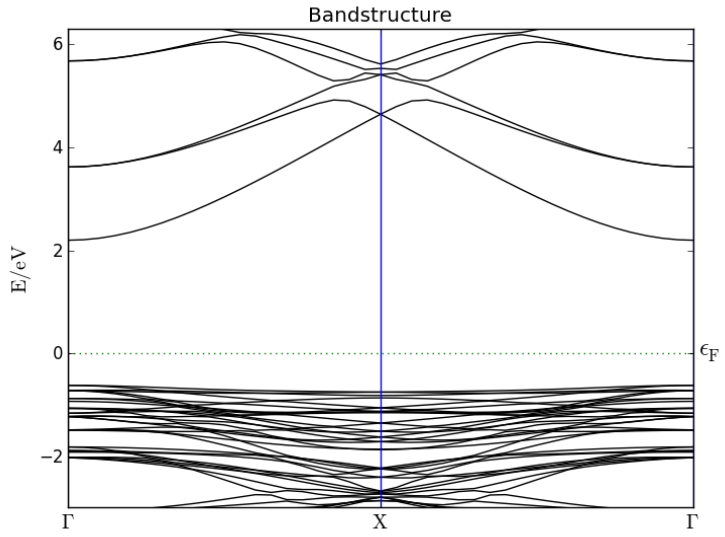

Figure 4: Electronic band structure of $NiFe_2O_4$ with Hubbard parameters of U = 5.0 eV for Fe 3d states and U = 6.0 eV for Ni 3d states.

where the $E[Zn\ /NiFe_2O_4](001)$ is the ground-state energy of the $NiFe_2O_4$ (001) surface with an adsorbed Zn atom. $E[Zn]$ is the ground-state energy of an isolated Zn atom, $E[NiFe_2O_4](001)$ is the ground-state energy of the pristine $NiFe_2O_4$ (001) surface. A negative value of E_{ads} indicates that the adsorption is exothermic (energetically favorable), while a positive value indicates an endothermic (energetically unfavorable) process.

Table 1: DFT SGGA PBE calculated zinc adsorption energies E_{ads}^{Zn} (eV) on the surface of a cubic crystal $NiFe_2O_4$ (001).

$NiFe_2O_4$ (001)		Surface Zn	
Site	$E_{ads}^{Zn}\ (eV)$	$d_{Zn-Ni(O)}(\AA)$	$d_{Zn-surf}(\AA)$
BS	-2.203	2.53	0.95
TS	-2.04	2.13	0.73
HS	-1.98	1.93	0.28

Table 2: Dependence of the Zn adsorption energy (E_{ads}^{Zn}) at the bridge site on the Zn–surface bond length and the height of the adsorbate above the $NiFe_2O_4$ (001) surface.

$NiFe_2O_4$ (001)		Surface Zn	
Adatom Zn on BS site	$E_{ads}^{Zn}\ (eV)$	$d_{Zn-Ni(Fe,O)}(\AA)$	$d_{Zn-surf}(\AA)$
Ni-Ni bond	-2.203	2.53	0.95
Ni-Fe bond	-1.72	2.04	0.51
O-O bond	-1.95	2.13	0.54

Table 3: DFT SGGA PBE calculated adsorption energy of Zn on $NiFe_2O_4$ (001) surface compared to E_{ads}^{Zn} of similar systems.

System	E_{ads}^{Zn}
Zn-$NiFe_2O_4$ (001) this work	-2.203eV
Zn- Zn (001) (Huang et al., 2022)	-1.35eV
Zn- Zn_xCu_y (001) (Meng et al., 2022)	-1.61eV
Zn- Cu41Sn11 (001) (Zhao et al., 2022)	-1.69eV

The adsorption energies of Zn atoms in three regions, taking into account the distance between the Zn atom and the $NiFe_2O_4$ atom (d_{Zn-Ni}) and the height of the adsorbate ($d_{Zn-surf}$),

are presented in Table 1-3. The adsorption energy between Zn adatom and $NiFe_2O_4$ surface depends on various factors, in particular, the bond length between the component atoms and the adatom position. When the bond length between Zn adatom and $NiFe_2O_4$ surface component atoms, in particular, the nickel atoms, is shorter, the adsorption energy of Zn is relatively greater (Table 1, 2). When the bond length between the adatom and the surface component atoms is long, physical adsorption may take place. Conversely, when the bond length is short, the adsorption energy raises due to chemical adsorption. Table 3 shows that the calculated adsorption energy of Zn on the $NiFe_2O_4$ (001) surface yields results comparable to those of Zn adsorbed on the GaAs (001) surface.

The following possible adsorption sites on the $NiFe_2O_4$ (001) surface were included in the scheme for calculating the adsorption energy of the Zn atom (Figure 5).

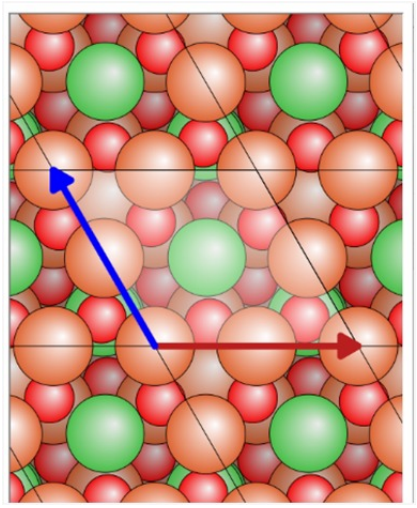

Figure 5: Crystal plane (001) of a cubic crystal with Miller indices.

Let us briefly consider how association occurs during metal adsorption on the surface of a magnetic ferrite. The association process during metal adsorption on the surface of magnetic ferrites can be understood in terms of the underlying physicochemical interactions between the adsorbent and the adsorbate. A precise understanding of the adsorption mechanism is critical, as the overall efficiency of the process is governed by the nature and strength of these interactions. $NiFe_2O_4$ has magnetic properties, allowing for: easy recovery of the adsorbent using magnets, reduction in secondary pollution, reusability, lowering long-term costs.

Adsorption is fundamentally a mass transfer phenomenon in which material migrates from the liquid phase to the solid surface through physical, chemical, or combined interactions. Physical adsorption (physisorption) originates from van der Waals forces associated with perturbations in the electronic configuration of the adsorbing species. In contrast, chemical adsorption (chemisorption) entails the formation of specific chemical bonds between surface-active sites of the adsorbent and the adsorbate. Due to the stronger interfacial interactions involved, chemisorption typically requires extended contact times to attain equilibrium, whereas physisorption proceeds relatively rapidly and reaches equilibrium within shorter time intervals.

(001) and mixed (110) surfaces with terminal oxygen groups of spinels exhibit stronger local interactions, for example, Zn-O (Rushiti et al., 2021). Considering this, only the (001) surface is studied.

The consideration of the magnetic properties of $NiFe_2O_4$ (Bouferrache et al., 2020; Yao et al., 2021) requires the solution of a special problem, in particular, with the study of conductivity and spin asymmetry and therefore will not be considered here.

4 Conclusion

In the present work, first-principles density functional theory calculations of the surface zinc atom adsorption behavior of Zn in the cubic crystal lattice of $NiFe_2O_4$ (001) were performed. We fulfilled calculations of the $NiFe_2O_4$ -Zn electronic structure using the DFT SGGA-PBE method. On the $NiFe_2O_4$ (001) surface three zinc adsorption sites were investigated: top, bridge, and hollow site in order to identify the most stable adsorption configuration and the nature of Zn–surface interactions.

The calculated adsorption energies illustrate that Zn adsorption on the $NiFe_2O_4$ (001) surface is energetically favorable for all considered configurations, with the hollow site exhibiting the strongest binding. The energetic stability of Zn adsorption at the hollow site is explained to the high coordination number between Zn and its nearest neighboring atoms, along with reduced electronic repulsion between the electron orbitals of the metal and zinc atoms. The adsorption energy of Zn at a HS site on the $NiFe_2O_4$ (001) surface practically constant (E^H_{ads}=-1.98eV). The negative adsorption energies and reduced Zn-O bond lengths indicate that Zn adsorption is governed predominantly by chemisorption. From the DOS spectra of $NiFe_2O_4$–Zn, it followed that the adsorption of Zn on the HS surface corresponded to chemical adsorption. Analysis of the total and partial density of states demostrates that Zn adsorption causes noticeable changes in the electronic structure near the Fermi level due to hybridization between Zn 3d states and O 2p, Fe 3d, and Ni 3d orbitals. The hollow-site configuration shows an enhancement of the electron states near the Fermi level, indicating stronger electronic interactions and a potential reduction in the band gap at the surface. These changes are expected to affect the surface reactivity and transport properties of $NiFe_2O_4$.

References

Adam, M.R., Othman, M.H.D., Kurniawan, T.A., Puteh, M.H., Ismail, A.F., Khongnakorn, W., ... & Jaafar, J. (2022). Advances in adsorptive membrane technology for water treatment and resource recovery applications: A critical review. *Journal of Environmental Chemical Engineering, 10*(3), 107633.

Asadov, S.M., Mustafaeva, S.N., & Mammadova, S.O. (2025). Modeling of hydrogen atom adsorption and diffusion in Ti3Sb intermetallic crystal with A15 cubic structure. *Surfaces, 8*(1), 17. https://doi.org/10.3390/surfaces8010017

Asadov, M.M., Mammadova, S.O., Huseynova, S.S., Mustafaeva, S.N., & Lukichev, V.F. (2023). Simulation of the adsorption and diffusion of lithium atoms on defective graphene for a Li-ion battery. *Russian Microelectronics, 52*(3), 167-185.

Asadov, M.M., Mustafaeva, S.N., Mammadova, S.O., Kuli-Zade, E.S., & Lukichev, V.F. (2024). Modeling of Structural Properties of Zr (Nb)-Doped c-LTO–Zr (Nb) Materials With Spinel Structure for Li-Ion Batteries. WSEAS Trans. *Electron*, 15, 166-183. https://doi.org/10.37394/232017.2024.15.19.

Bouferrache, K., Charifi, Z., Baaziz, H., Alsaad, A.M., & Telfah, A. (2020). Electronic structure, magnetic and optic properties of spinel compound NiFe2O4. *Semiconductor Science and Technology, 35*(9), 095013. https://doi.org/10.1088/1361-6641/ab9845

Dileep, K., Loukya, B., Pachauri, N., Gupta, A., & Datta, R. (2014). Probing optical band gaps at the nanoscale in $NiFe_2O_4$ and $CoFe_2O_4$ epitaxial films by high resolution electron energy loss spectroscopy. *Journal of Applied Physics, 116*(10), https://doi.org/10.1063/1.4895059.

Farhan, A., Arshad, J., Rashid, E.U., Ahmad, H., Nawaz, S., Munawar, J., ... & Bilal, M. (2023). Metal ferrites-based nanocomposites and nanohybrids for photocatalytic water treatment and electrocatalytic water splitting. *Chemosphere*, 310, 136835.

Gonçalves, J.M., de Faria, L.V., Nascimento, A.B., Germscheidt, R.L., Patra, S., Hernández-Saravia, L.P., ... & Angnes, L. (2022). Sensing performances of spinel ferrites MFe2O4 (M= Mg, Ni, Co, Mn, Cu and Zn) based electrochemical sensors: A review. *Analytica Chimica Acta*, 1233, 340362.

Huang, Z., Li, H., Yang, Z., Wang, H., Ding, J., Xu, L., ... & Hu, W. (2022). Nanosecond laser lithography enables concave-convex zinc metal battery anodes with ultrahigh areal capacity. *Energy Storage Materials*, 51, 273-285.

Kefeni, K.K., Mamba, B.B., & Msagati, T.A. (2017). Application of spinel ferrite nanoparticles in water and wastewater treatment: a review. *Separation and Purification Technology*, 188, 399-422.

Kefeni, K.K., Mamba, B.B. (2020). Photocatalytic application of spinel ferrite nanoparticles and nanocomposites in wastewater treatment. *Sustainable Materials and Technologies*, 23, e00140.

Leonel, A.G., Mansur, A.A., & Mansur, H.S. (2021). Advanced functional nanostructures based on magnetic iron oxide nanomaterials for water remediation: a review. *Water research*, 190, 116693.

Malaie, K., Ganjali, M.R. (2021). Spinel nano-ferrites for aqueous supercapacitors; linking abundant resources and low-cost processes for sustainable energy storage. *Journal of Energy Storage*, 33, 102097.

Meng, H., Ran, Q., Dai, T.Y., Shi, H., Zeng, S.P., Zhu, Y. F., ... & Jiang, Q. (2022). Surface-alloyed nanoporous zinc as reversible and stable anodes for high-performance aqueous zinc-ion battery. *Nano-Micro Letters, 14*(1), 128.

Narang, S.B., Pubby, K. (2021). Nickel spinel ferrites: a review. *Journal of Magnetism and Magnetic Materials,* 519, 167163.

Nithya, R., Thirunavukkarasu, A., Sathya, A.B., & Sivashankar, R. (2021). Magnetic materials and magnetic separation of dyes from aqueous solutions: a review. *Environmental Chemistry Letters, 19*(2), 1275-1294.

Nnadozie, E.C., Ajibade, P.A. (2020). Multifunctional magnetic oxide nanoparticle (MNP) core-shell: review of synthesis, structural studies and application for wastewater treatment. *Molecules, 25*(18), 4110.

Rushiti, A., Hättig, C., Wen, B., & Selloni, A. (2021). Structure and reactivity of pristine and reduced spinel $CoFe_2O_4$ (001)/(100) surfaces. The Journal of Physical Chemistry C, 125(18), 9774-9781. https://doi.org/10.1021/acs.jpcc.1c01881

Salih, S.J., Mahmood, W.M. (2023). Review on magnetic spinel ferrite (MFe2O4) nanoparticles: From synthesis to application. *Heliyon, 9*(6).

Sidorowicz, A., Yigit, N., Wicht, T., Stöger-Pollach, M., Concas, A., Orrù, R., ... & Rupprechter, G. (2024). Microalgae-derived Co 3 O 4 nanomaterials for catalytic CO oxidation. *RSC advances, 14*(7), 4575-4586.

Srinivasan, S.Y., Paknikar, K.M., Bodas, D., & Gajbhiye, V. (2018). Applications of cobalt ferrite nanoparticles in biomedical nanotechnology. *Nanomedicine, 13*(10), 1221-1238.

Yao, H., Ning, X., Zhao, H., Hao, A., & Ismail, M. (2021). Effect of Gd-doping on structural, optical, and magnetic properties of NiFe2O4 as-prepared thin films via facile sol–gel approach. *ACS omega, 6*(9), 6305-6311, https://doi.org/10.1021/acsomega.0c06097

Zohrabi, Y. (2024). Synthesis and application of magnetic ferrites (MFe2O4) in the removal of heavy metals from aqueous solutions: an updated review. *Materials Science and Engineering: B,* 299, 117024.

Zhao, Q., Liu, W., Chen, Y., & Chen, L. (2022). Ultra-stable Zn metal batteries with dendrite-free Cu-Sn alloy induced high-quality composite Zn mesh. *Chemical Engineering Journal, 450, 137979.*